NMRlipids IV: Headgroup & glycerol backbone structures, and cation binding in bilayers with PE and PG lipids

Amélie Bacle,[1] Pavel Buslaev,[2] Rebeca García Fandiño,[3,4] Fernando Favela-Rosales,[5] Tiago Ferreira,[6] Patrick Fuchs,[1] Ivan Gushchin,[7] Matti Javanainen,[8] Anne M. Kiirikki,[9] Jesper J. Madsen,[10,11] Josef Melcr,[8,12] Paula Milan Rodriguez,[1] Markus S. Miettinen,[13] O. H. Samuli Ollila,[9,*] Chris G. Papadopoulos,[14] Antonio Peón,[15] Thomas J. Piggot,[16] and Ángel Piñeiro[17]

[1]*Paris, France*
[2]*University of Jyväskylä*
[3]*Center for Research in Biological Chemistry and Molecular Materials (CiQUS), Universidade de Santiago de Compostela, E-15782 Santiago de Compostela, Spain*
[4]*CIQUP, Centro de Investigao em Qumica, Departamento de Qumica e Bioqumica, Faculdade de Ciłncias, Universidade do Porto, Porto, Portugal*
[5]*Departamento de Ciencias Básicas, Tecnológico Nacional de México, Campus Zacatecas Occidente, México*
[6]*Halle, Germany*
[7]*Moscow Institute of Physics and Technology, Dolgoprudny, Russia*
[8]*Institute of Organic Chemistry and Biochemistry of the Czech Academy of Sciences, Flemingovo nám. 542/2, CZ-16610 Prague 6, Czech Republic*
[9]*Institute of Biotechnology, University of Helsinki*
[10]*Department of Chemistry, The University of Chicago, Chicago, Illinois, United States of America*
[11]*Department of Global Health, College of Public Health, University of South Florida, Tampa, Florida, United States of America*
[12]*Groningen Biomolecular Sciences and Biotechnology Institute and The Zernike Institute for Advanced Materials, University of Groningen, 9747 AG Groningen, The Netherlands*
[13]*Department of Theory and Bio-Systems, Max Planck Institute of Colloids and Interfaces, 14424 Potsdam, Germany*
[14]*I2BC - University Paris Sud*
[15]*Spain*
[16]*Chemistry, University of Southampton, Highfield, Southampton SO17 1BJ, United Kingdom*
[17]*Departamento de Física Aplicada, Facultade de Física, Universidade de Santiago de Compostela, E-15782 Santiago de Compostela, Spain*

(Dated: March 17, 2021)

Chemistry of lipid headgroups, the water facing components of cell membranes that regulate cell functions via lipid–protein interactions, varies between organisms and organelles. Because lipid membranes are in liquid state under physiological conditions, the conformational ensembles of different lipid headgroups are difficult to resolve experimentally. Here, we combine solid state NMR experiments and molecular dynamics simulations from NMRlipids open collaboration to resolve the conformational ensembles of the headgroups of key lipid types in liquid lamellar phase under various biologically relevant conditions. Interpretation of NMR experiments using the plethora of simulation data collected in the NMRlipids project suggests that all lipid headgroups sample a wide range of conformations in neutral and charged cellular membranes. However, the populations of different conformations are dictated by the headgroup chemistry. Together with the analysis of protein-bound lipids from the protein data bank (PDB), this suggests that lipids can bind to proteins in wide range of conformations independently on the headgroup chemistry. Therefore, the selective adsorption of proteins to membranes is likely regulated by specific protein–lipid interactions, rather than conformational restrictions of lipids. Our results pave the way to comprehensive understanding of lipid–protein interaction energetics, and the understanding of complex biomolecular assemblies such as membrane proteins.

INTRODUCTION

Chemical compositions of hydrophilic lipid headgroups vary between different organelles and organisms, and different lipid types regulate protein functions in many different ways [1, 2]. Lipids can directly bind to proteins or indirectly affect protein functions by altering membrane properties such as charge or elasticity [1, 3]. While the specific interactions with certain lipid headgroups are known to be essential for the function of several proteins [3, 4], it is not clear if the specificity is driven by the differences in accessible conformational states between lipid types or by specific intermolecular lipid–protein interactions.

The conformational ensembles of lipids in the physiologically relevant lamellar liquid phase are typically derived from NMR experiments, particularly from C–H bond order parameters measured using ^{2}H NMR [5–7]. Notably, such measurements can be performed also on living cells [8–10]. These studies suggest that the glycerol backbone conformations are largely similar irrespectively of the headgroup [8], and the headgroup conformations are similar in phosphatidylcholine (PC), phosphatidylethanolamine (PE) and phosphatidylglycerol (PG) lipids, while the headgroup is more rigid in phosphatidylserine (PS) lipids [11, 12]. However, these tendencies are based only on the absolute values, whereas the necessity of order parameter signs in capturing the conformational ensembles of lipids has been recently demonstrated [13–15].

Furthermore, the detailed understanding of lipid conformational ensembles is limited by the lack of universal models that would map order parameters to structural ensembles [16, 17].

Stuctures of different lipid types in protein bound states can be extracted from the protein data bank (PDB) [18], but their relation to the conformational ensembles in liquid lamellar state remains unclear [19]. In addition to the changes in lipid conformational ensembles upon binding to proteins, also the experimentally measured response of lipid headgroup to membrane bound charges remains poorly understood due to the lack of suitable models to interpret the lipid conformational ensembles in liquid lamellar state [7].

Here, we use natural abundance ^{13}C NMR experiments and MD simulations from the NMRlipids open collaboration to resolve the differences in conformational ensembles between PC, PE, PG and PS lipid headgroups. Zwitterionic PC and PE are the most common lipids in eukaryotes and bacteria, respectively [2, 20]. PE is also the second most abundant glycerophospholipid in eukaryotic cells and has been related to various diseases [21–23]. PS and PG are the most common negatively charged lipids in eukaryotes and bacteria, respectively, and affect membrane protein functionality and signaling [3, 20, 24, 25]. All the studied lipids specifically bind to various proteins [26]. We use our results to elucidate also lipid–protein interactions and the effect of charges on lipid conformations.

The lipid conformational ensembles in liquid lamellar state paves the way toward understanding the specific binding of different lipid types to membrane proteins and how they regulate the protein function. Because glycerol backbone and headgroup structures of PC lipids are similar in model membranes and in bacteria [8–10], the results from model systems could be used to understand the biological role of lipid headgroup conformational ensembles in different lipid types.

METHODS

Experimental C–H bond order parameters

The headgroup and glycerol backbone C–H bond order parameters of 1-palmitoyl-2-oleoyl-sn-glycero-3-phosphoethanolamine (POPE) and 1-palmitoyl-2-oleoyl-sn-glycero-3-phospho-(1'-rac-glycerol) (POPG), purchased from Avanti polar lipids, were measured using natural abundance ^{13}C solid state NMR spectroscopy as described previously [15, 27]. The magnitudes of order parameters were determined from the chemical-shift resolved dipolar splittings using a R-type Proton Detected Local Field (R-PDLF) experiment [28] and the signs from S-DROSS experiments [29] combined with SIMPSON simulations [30]. The NMR experiments were identical as in our previous work [31]. The POPE experiments were recorded at 310 K and POPG experiments at 298 K, where the bilayers are in the liquid disordered phase [32].

Glycerol backbone peaks from both lipids, and α-carbon peak from POPE in the INEPT spectra were assigned based on previously measured POPC spectra [27]. The β-carbon peak from POPE was assigned based on ^{13}C chemical shift table for amines available at `https://www.chem.wisc.edu/areas/reich/nmr/c13-data/cdata.htm`. **1.How were α and γ-carbon peaks assigned in POPG?**. The β-carbon peak from POPG overlapped with the g_2 peak from glycerol backbone because their chemical environments are similar. **2.Details to be checked by Tiago**.

Molecular dynamics simulations

Molecular dynamics simulation data were collected and analyzed using the methods from the NMRlipids Open Collaboration project (`nmrlipids.blogspot.fi`) [13, 14, 31, 33]. Simulation and accessibility details of more than 70 systems simulated for this work are given in the supplementary information. Quality evaluation of these simulations enables us to select the best models for the interpretation of lipid conformational ensembles from the experimental data.

The quality of lipid headgroup and glycerol backbone conformational ensembles in PE and PG simulations were evaluated using the C-H bond order parameters [13]. Interactions between different headgroups in simulations of mixed bilayers were evaluated monitoring the changes in headgroup order parameters upon mixing the lipids [31]. The ion binding affinities and response of lipids to bound charge were evaluated monitoring the changes of lipid headgroup order parameters [31, 33].

Analysis of conformations of protein-bound lipids

Lipid structures from Protein Data Bank (PDB, `http://www.rcsb.org/`) were searched using PDBe REST API (`www.ebi.ac.uk/pdbe/pdbe-rest-api`) using the ligand names listed in the supplementary information. Heavy atom dihedral distributions from the lipid structures were calculated using the MDAnalysis python library [37, 38] and Jupyter notebook available from `https://github.com/pbuslaev/scr/blob/master/PDB%20analysis.ipynb`. Only structures from X-ray and Cryo-EM with higher than 3.2 Å resolution were used in the analysis. Lipids from same PDBID with all dihedrals angles within 3 degrees were discarded from the analysis to avoid overweighting of lipid structures present, e.g., due to rotational symmetries.

To demonstrate the existence of similar structures of different lipids bound to different proteins, we searched pairs having the last five dihedral angles (excluding g_1-g_2-g_3-O_{g3}) within 30 degrees from structures with resolution higher than 2.5 Å. The two most representative examples were hand-picked from the results.

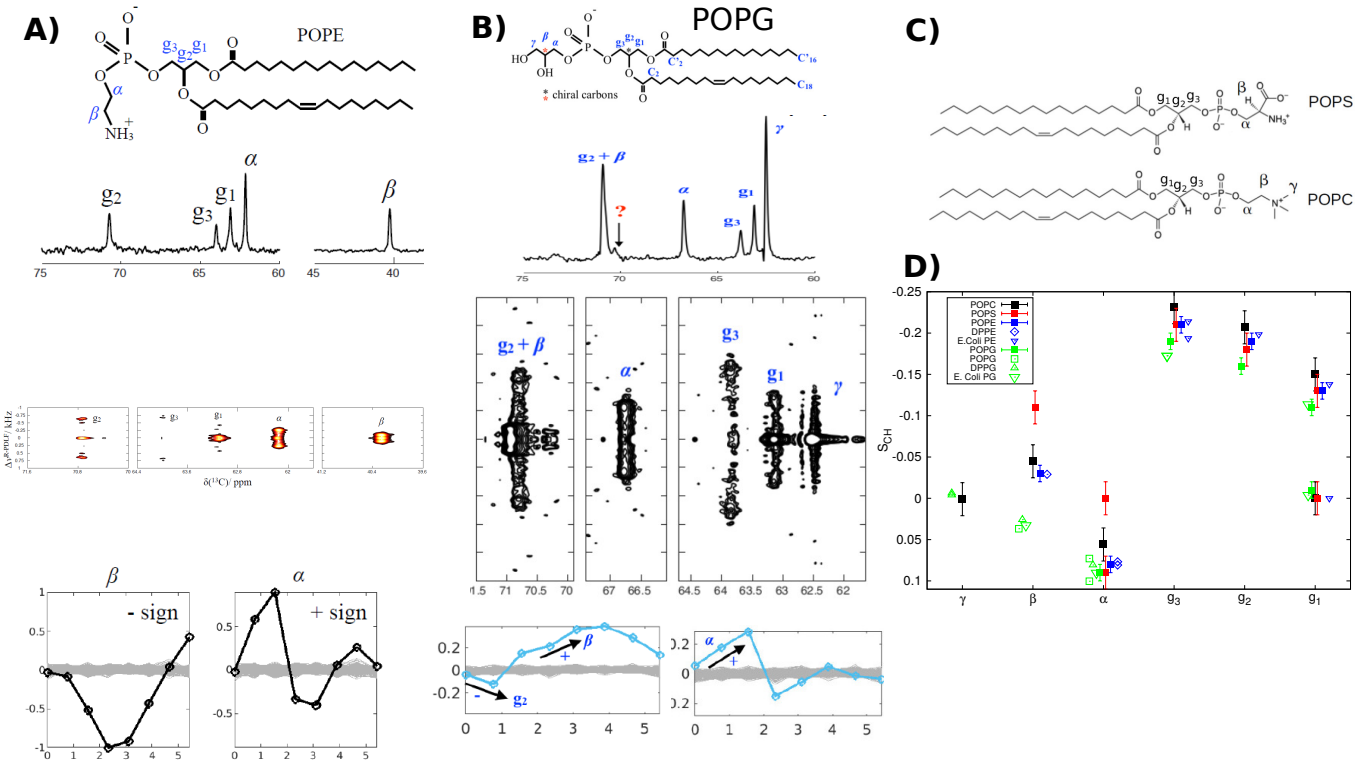

FIG. 1: Chemical structure, refocused-INEPT spectrum, 2D R-PDLF spectra, and S-DROSS data (from top to bottom) of **A)** POPE and **B)** POPG. Full NMR spectra are shown Figs. S1 and S2. **C)** Chemical structure of POPC and POPS. **D)** Headgroup and glycerol backbone order parameters from different experiments in lamellar liquid disordered phase. The values and signs for POPE (310 K) and POPG (298 K) measured in this work, and for POPS (298 K) [31] and POPC (300 K) [15, 27] previously using ^{13}C NMR. The literature values for DOPS with 0.1M of NaCl (303 K) [34], POPG with 10nM PIPES (298 K) [35], DPPG with 10mM PIPES and 100mM NaCl (314 K) [11], DPPE (341 K) [36], E.coliPE and E.coliPG (310 K) [8] are measured using ^{2}H NMR. The signs from ^{13}C NMR are used also for the literature values.

3.This is a sketch, Tiago Ferreira will make a new figure.

RESULTS AND DISCUSSION

Differences between lipid headgroups in bulk bilayer from ^{13}C NMR experiments

To experimentally characterize the headgroup conformational ensembles of lipids that are not bound to proteins in an electrostatically neutral cell membrane, we measured the C–H bond order parameters and their signs of POPG and POPE in the liquid lamellar phase, as we did previously for POPC and POPS [15, 27, 31]. Determination of headgroup and glycerol backbone order parameters and their signs was straightforward from the data in Figs. 1, S1 and S2 for all the C–H bonds, except for the β and g_2 carbons in POPG. These carbons have overlapping peaks in the INEPT spectra due to their similar chemical environments, and only the magnitude of the larger order parameter could be determined from the R-PDLF spectra (Fig. 1B)). Nevertheless, based on previous ^{2}H NMR measurements [8, 11, 35], we assigned the larger order parameter to the g_2 carbon and used the literature value for the β-carbon in SIMPSON simulations to determine the signs. The decrease in the beginning of the S-DROSS curve suggests that the sign of larger g_2 order parameter is negative and later increase suggests that sign of smaller β order parameter is positive (Fig. 1B)). This interpretation is confirmed by SIMPSON calculations in Fig. S3.

Experimental order parameters of POPC, POPE, POPG and POPS glycerol backbones and headgroups from this and previous studies are collected in Fig. 1D), where signs determined from ^{13}C NMR experiments are used also for the ^{2}H NMR data from the literature. The overall agreement of order parameters determined by different research teams and different techniques for the same lipid headgroup is very good here and in previous studies [13, 14, 31]. This suggests that the observed differences between lipid types arise from differences in headgroup chemistry rather than inaccuracies in experiments, or differences in the acyl chains or in experimental conditions. The most distinct order parameters are observed for PS headgroups, for which the α-carbon order parameter exhibits significant forking and the β-carbon has more negative value than other studied lipid types. On the other hand, the β-carbon order parameter of PG headgroup has a positive sign, in contrast to all the other lipid types. Notably, this has not been observed in traditional ^{2}H NMR experiments, where only the absolute value of the order parameters are measured [8, 11, 35]. The glycerol backbone order parameters are

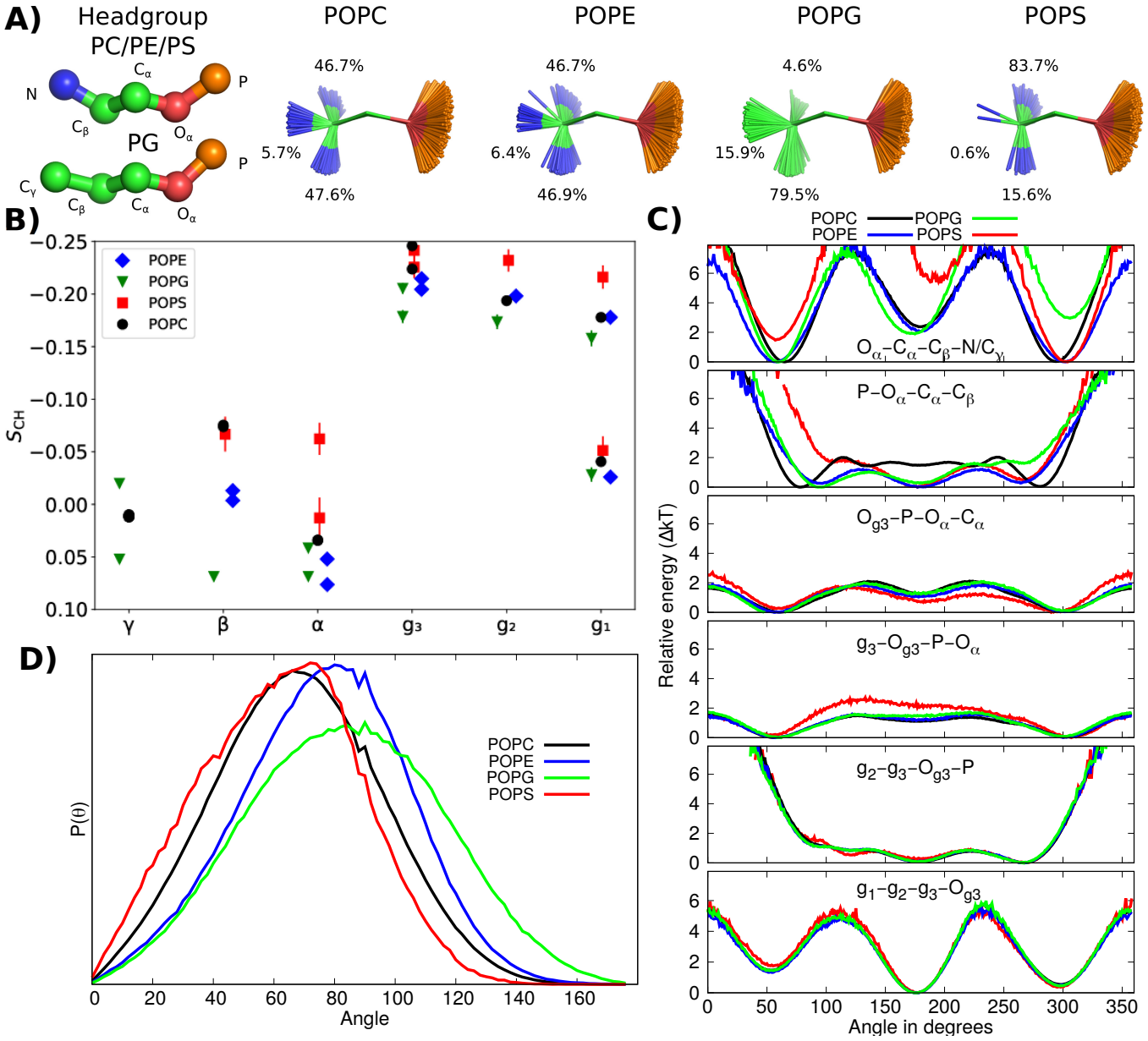

FIG. 2: Results from the best simulation model (CHARMM36) simulations demonstrating the differences in conformational ensembles between different lipids. **A)** Snapshots with overlayed C_β, C_α and O_α atoms and occurence of different conformations. **B)** Headgroup and glycerol backbone region order parameters of different different lipids. **C)** Relative energies for individual dihedral angles estimated from inverse Boltzmann distributions of heavy atom dihedral angles. The states corresponding energies higher than 7 kT are not shown because they are not observed in simulations. **D)** Distributions of P-N vector angle with respect to membrane normal.

similar for all the lipid types, although they move slightly toward positive values (closer to zero) in the order PC < PE < PS < PG. Essential differences between PC and PE headgroups are not observed.

Conformational ensembles of different lipid headgroups in bulk bilayer from MD simulations

To understand the structural origin of distinct order parameters for PG and PS lipids, we first calculated the heavy atom dihedral angle distributions from simulations that best reproduce the differences between headgroups according to the quality evaluation in the SI and Refs. [13, 31] (Fig. S12). Then, we used the inverse Boltzmann distributions to estimate the energy costs for different dihedral angle orientations. The

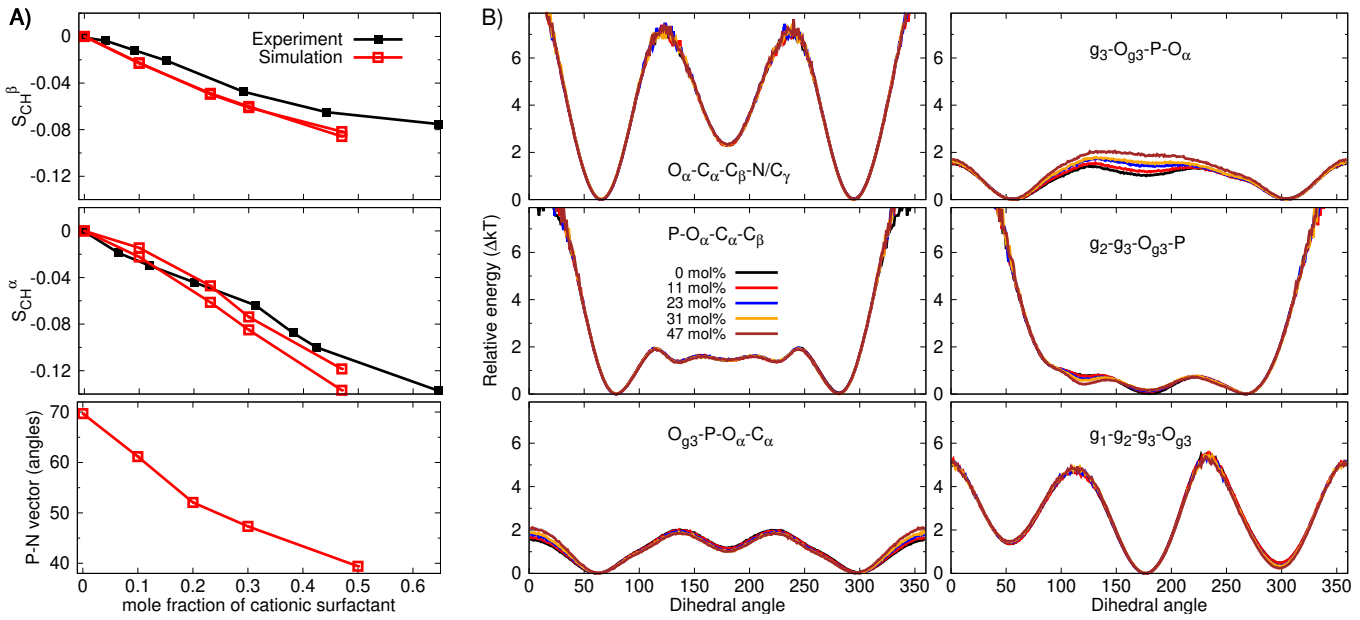

FIG. 3: **A)** Modulation of PC headgroup order parameters and P–N vector angle upon addition of cationic surfactant from CHARMM36 simulations compared with the experimental data [39]. **B)** Relative energies for individual dihedral angles estimated from inverse Boltzmann distributions of heavy atom dihedral angles with different amounts of cationic surfactant from CHARMM36 simulations.

results in Fig. 2C) suggest that all lipid headgroups are very flexible and energy costs for rotating individual dihedrals to almost any angle is low (below 7 kT). Only *cis* states of P-O_α-C_α-C_β and g_2-g_3-O_{g_3}-P have larger relative energies and are not observed for any lipids during the simulations.

Major differences between headgroups are observed for the last two dihedrals in the headgroup end, O_α-C_α-C_β-N/C_γ and P-O_α-C_α-C_β, which prefer *gauche*$^-$ conformations for PG and *gauche*$^+$ for PS, while PC and PE exhibit symmetric distributions. Also, the energy barriers for O_α-C_α-C_β-N/C_γ dihedral rotations between *gauche* and *trans* states are larger for PS and PG lipids than for PC and PE lipids. Rest of the dihedrals are similar between different lipids, with the exception of PS lipids for which slightly larger energy for ecplised anti conformation in g_3-O_{g3}-P-O_α dihedral was observed. Therefore we suggest that the main differences between lipid headgroups leading to distinct order parameter occur in the choline part, while also changes in phosphate region may contribute in PS lipids. The increased barriers for dihedral rotations may explain the more rigid headgroup structures in PS [12, 34]. Furthermore, the angle between headgroup dipole and membrane normal decreases in the order of PG > PE > PC > PS (Fig. 2D)). However, the differences between PC and PE in P-O_α-C_α-C_β dihedral and P–N vector dipole may be artificial as the β-carbon order parameter in PC is too negative in the CHARMM36 force field, thereby not being equal to the order parameter in PE as observed in experiments [13].

In conclusion, all lipid headgroups sample very broad conformational ensembles in liquid lamellar phase and sampled dihedral angles are within approximately same ranges for all headgroup types. Because the rotation of dihedral angles to almost any position bears relatively low energy cost, the lipid headgroups are able to adopt wide range of multiple conformations when interacting with proteins, ions or other biomolecules. The wide range of observed conformations suggest that the structures in lipid crystals [12, 40] play only a minor role, and that the models aiming to explain NMR data using only few conformations [5–7, 17] are not sufficient to capture the large conformational space of lipids in liquid lamellar state.

Lipid conformational ensembles in lipid bilayers with bound ions

Charged entities, such as lipids, proteins, surfactants, drugs, and ions incorporated in membranes reorient the headgroup dipole in PC lipids, thereby affecting the order parameters of lipid headgroups [41]. However, the detailed understanding on structural and energetic response of lipids to membrane bound electric charge is still lacking [7].

To resolve lipid headgroup conformational ensembles in cell membrane bearing positive charge, we calculated the heavy atom dihedral angle distributions from simulations that correctly captured the experimentally measured decrease in PC headgroup order parameters upon addition of cationic surfactants into a bilayer in figure 3 A). The dihedral angle distributions and relative energies in figures S13 and 3 B reveal that the addition positive charge into a membrane decrease the abundance of trans states in g_2-g_3-O_{g_3}-P and g_3-O_{g_3}-P-O_α dihedrals. Choline region remains essentially unchanged and only minor changes are observed in other dihedrals even

though almost half of the molecules in membranes are cationic surfactants.

Also binding of ions to membranes may affect the lipid headgroup conformational ensembles in physiological conditions. The bound Ca^{2+} ion to PC headgroup leads to similar decrease in trans state probability for g_3-O_{g3}-P-O_α dihedral as observed for cationic surfactants in the most realistic MD simulations models (lipid17ecc and CHARMM36 in Figs. S14, S15 and Fig. S8). The dihedral distributions of PG headgroup are more sensitive to the bound ions in the most realistic simulations, but upward tilting of the headgroup dipole upon addition of $CaCl_2$ is weaker than in PC (Lipid17 and Slipids in Figs. S8, S16 and S17). However, the changes in PG lipid dihedrals upon addition of $CaCl_2$ differ between the best models (Figs. S16 and S17), none of the simulations captures the Ca^{2+} ion binding affinity and conformational ensemble of PG lipids simultaneously, and experimental data to evaluate the response of α-carbon order parameters to the added $CaCl_2$ in PG is not available. Also the headgroup conformational ensembles in mixtures of PC and charged (PG or PS) or zwitterionic (PE) lipids could not be resolve with the currently available force fields and experimental data (Figs. S6 and S7, and Ref. [31, 42]).

Despite the difficulties in simulations to capture the headgroup conformations in mixtures involving charged lipids, we can conclude that the structural response of lipid headgroups to membrane bound charges arise from relatively small changes in conformational ensembles. These changes eventuate from mild changes in dihedral angle distributions, rather than from restriction of lipids into fixed conformations. Therefore, lipid headgroups remain in disordered state sampling large space of different conformations also in charged membranes, thereby being able to interact with different molecules in multiple ways.

Protein-bound lipid conformations

Interpretation of experimental order parameters using MD simulations in previous sections suggest that PC, PE, PG and PS lipid headgroups are very flexible, thereby being able to bind proteins in various different conformations. To test this prediction, we analyzed the protein bound lipid conformations from structures deposited in the PDB [18]. We found 311 PC, 394 PE, 154 PG, and 35 PS conformations presenting lipids that are tightly bound to proteins in fixed conformations that were determined as a part of protein structure using crystallography or cryo-EM.

The heavy atom dihedral angle distributions calculated from these conformations in Fig. 4 A) reveal that the protein bound lipids indeed exhibit wide range of conformations independently on the headgroup type. As in bulk lipid bilayers, only cis conformations of P-O_α-C_α-C_β and g_2-g_3-O_{g_3}-P dihedrals are almost completely restricted in all lipids, and significant differences between different headgroups were not observed. Structures deviating from lipid crystals have been previously proposed to indicate inaccuracies in lipid structures in PDB [16, 19]. However, we see large deviations from lipid crystals structures also in conformational ensembles that reproduce the NMR data in liquid lamellar phase, thereby proposing that such deviations are realistic also in protein-bound states.

Our results suggest that flexible lipid headgroups can optimize the intermolecular interactions with proteins by binding in wide range of conformations. Therefore, the specific binding of lipids to proteins is not driven by the structural differences between headgroups. This is demonstrated in Fig. 4 B) with two examples where different lipids bound to different proteins have identical conformations: PE in cytochrome bc_1 complex is similar to PC bound to yeast sec14, and PG bound to bovine cytochrome *c* oxidase is similar to PC bound to pore-forming toxin (FraC). On the other hand, a single lipid headgroup type is cabable to adapt itself to various binding positions, thereby being able to specifically bind to many different kinds of binding sites in different proteins.

CONCLUSIONS

C-H bond order parameters from NMR experiments suggest that lipid headgroup conformational ensembles depend on lipid type (PC, PE, PG or PS) and accumulated membrane charge (cationic lipids, surfactants, ions or drugs). Our interpretation of this data, using massive amount of simulations collected within the NMRlipids open collaboration, revealed that the differences in order parameters can be explained by relatively small changes in dihedral angle probability distributions. All studied headgroups (PC, PE, PG and PS) are flexible and access similar wide range of conformations with only very few resticted dihedral orientations also when charges are bound to membranes. The observed differences in order parameters originate from reweighting conformational probabilities rather than changes in accessible structures.

The flexibility and wide conformational space of headgroups suggest that protein bound lipids can adapt to various binding sites to optimize the intermolecular lipid–protein interactions. We tested this prediction by analyzing the conformations of lipids that are tightly bound to proteins in from PDB. Indeed, also protein bound lipids exhibit wide range of conformations without significant differences between different lipid types. Therefore, the specificify of lipid binding to proteins is not regulated by accessible structures of lipids, and a single lipid type can adapt to various binding sites in proteins.

Our results pave the way toward understanding of lipid mediated cell signaling and how lipids regulate membrane protein function in general. We suggest that the key to understand selective binding of certain lipid types to proteins are intermolecular lipid-protein interactions, rather than conformational restrictions of lipids. On the other hand, wide conformational ensembles in bulk bilayers suggest that lipid crystal structures play a minor role and that entropic cost of lipid

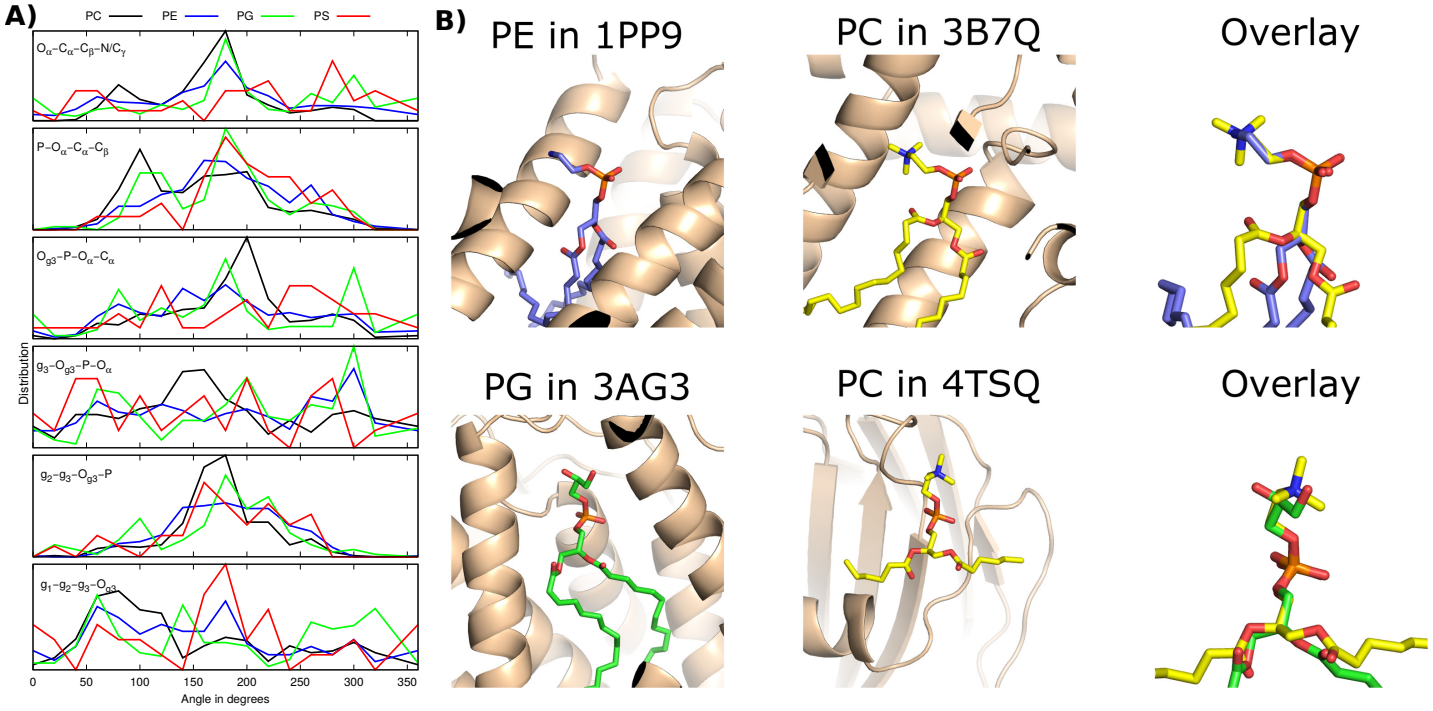

FIG. 4: A) Dihedral distributions fromm lipid structures in PDB. B) PE headgroup bound to cytochrome bc_1 complex (1PP9 [43]) with identical conformation as PC headgroup to yeast sec14 (3B7Q [44]), and PG headgroup bound to bovine cytochrome c oxidase (3AG3 [45]) as PC to FraC, a pore-forming toxin (4TSQ [46]).

binding may be significant. Finally, the results demonstrate the power of open access MD simulations collected in NMRlipids open collaboration to complement PDB in order to understand functions of complex systems containing disordered biomolecules.

AP is grateful to the Centro de Supercomputacin de Galicia (CESGA) for use of the Finis Terrae computer

* samuli.ollila@helsinki.fi

[1] A. Lee, Biochimica et Biophysica Acta (BBA) - Biomembranes **1612**, 1 (2003), ISSN 0005-2736, URL http://www.sciencedirect.com/science/article/pii/S0005273603000567.

[2] G. van Meer, D. R. Voelker, and G. W. Feigenson, Nature Reviews Molecular Cell Biology **9**, 112 (2008), URL https://doi.org/10.1038/nrm2330.

[3] M. A. Lemmon, Nat. Rev. Mol. Cell Biol. **9**, 99 (2008).

[4] A. G. Lee, Trends in Biochemical Sciences **36**, 493 (2011), URL https://doi.org/10.1016/j.tibs.2011.06.007.

[5] J. Seelig, Q. Rev. Biophys. **10**, 353 (1977).

[6] J. H. Davis, Biochim. Biophys. Acta **737**, 117 (1983).

[7] D. J. Semchyschyn and P. M. Macdonald, Magn. Res. Chem. **42**, 89 (2004).

[8] H. U. Gally, G. Pluschke, P. Overath, and J. Seelig, Biochemistry **20**, 1826 (1981).

[9] P. Scherer and J. Seelig, EMBO J. **6** (1987).

[10] J. Seelig, Cell Biology International Reports **14**, 353 (1990), ISSN 0309-1651, URL http://www.sciencedirect.com/science/article/pii/030916519091204H.

[11] R. Wohlgemuth, N. Waespe-Sarcevic, and J. Seelig, Biochemistry **19**, 3315 (1980).

[12] G. Büldt and R. Wohlgemuth, The Journal of Membrane Biology **58**, 81 (1981), ISSN 1432-1424, URL http://dx.doi.org/10.1007/BF01870972.

[13] A. Botan, F. Favela-Rosales, P. F. J. Fuchs, M. Javanainen, M. Kanduč, W. Kulig, A. Lamberg, C. Loison, A. Lyubartsev, M. S. Miettinen, et al., J. Phys. Chem. B **119**, 15075 (2015).

[14] O. S. Ollila and G. Pabst, Biochimica et Biophysica Acta (BBA) - Biomembranes **1858**, 2512 (2016).

[15] T. M. Ferreira, R. Sood, R. Bärenwald, G. Carlström, D. Topgaard, K. Saalwächter, P. K. J. Kinnunen, and O. H. S. Ollila, Langmuir **32**, 6524 (2016).

[16] W. Pezeshkian, H. Khandelia, and D. Marsh, Biophysical Journal **114**, 1895 (2018), ISSN 0006-3495, URL http://www.sciencedirect.com/science/article/pii/S0006349518302467.

[17] H. Akutsu, Biochimica et Biophysica Acta (BBA) - Biomembranes **1862**, 183352 (2020), URL https://doi.org/10.1016/j.bbamem.2020.183352.

[18] H. M. Berman, J. Westbrook, Z. Feng, G. Gilliland, T. N. Bhat, H. Weissig, I. N. Shindyalov, and P. E. Bourne, Nucleic Acids Research **28**, 235 (2000), ISSN 0305-1048, https://academic.oup.com/nar/article-pdf/28/1/235/9895144/280235.pdf, URL https://doi.org/10.1093/nar/28.1.235.

[19] D. Marsh and T. Páli, European Biophysics Journal **42**, 119 (2013), URL https://doi.org/10.1007/s00249-012-0816-6.

[20] C. Sohlenkamp and O. Geiger, FEMS Microbiology Reviews

40, 133 (2015).
[21] J. E. Vance, Traffic **16**, 1 (2015).
[22] E. Calzada, O. Onguka, and S. M. Claypool (Academic Press, 2016), vol. 321 of *International Review of Cell and Molecular Biology*, pp. 29 – 88.
[23] D. Patel and S. N. Witt, Oxidative Medicine and Cellular Longevity **2017**, 4829180 (2017).
[24] P. A. Leventis and S. Grinstein, Annual Review of Biophysics **39**, 407 (2010).
[25] P. Hariharan, E. Tikhonova, J. Medeiros-Silva, A. Jeucken, M. V. Bogdanov, W. Dowhan, J. F. Brouwers, M. Weingarth, and L. Guan, BMC Biology **16**, 85 (2018).
[26] P. L. Yeagle, Biochimica et Biophysica Acta (BBA) - Biomembranes **1838**, 1548 (2014), membrane Structure and Function: Relevance in the Cell's Physiology, Pathology and Therapy.
[27] T. M. Ferreira, F. Coreta-Gomes, O. H. S. Ollila, M. J. Moreno, W. L. C. Vaz, and D. Topgaard, Phys. Chem. Chem. Phys. **15**, 1976 (2013).
[28] S. V. Dvinskikh, H. Zimmermann, A. Maliniak, and D. Sandstrom, J. Magn. Reson. **168**, 194 (2004).
[29] J. D. Gross, D. E. Warschawski, and R. G. Griffin, J. Am. Chem. Soc. **119**, 796 (1997).
[30] M. Bak, J. T. Rasmussen, and N. C. Nielsen, Journal of Magnetic Resonance **147**, 296 (2000), ISSN 1090-7807, URL http://www.sciencedirect.com/science/article/pii/S1090780700921797.
[31] H. S. Antila, P. Buslaev, F. Favela-Rosales, T. Mendes Ferreira, I. Gushchin, M. Javanainen, B. Kav, J. J. Madsen, J. Melcr, M. S. Miettinen, et al., The Journal of Physical Chemistry B p. acs.jpcb.9b06091 (2019), ISSN 1520-6106.
[32] D. Marsh, *Handbook of Lipid Bilayers, Second Edition* (RSC press, 2013).
[33] A. Catte, M. Girych, M. Javanainen, C. Loison, J. Melcr, M. S. Miettinen, L. Monticelli, J. Maatta, V. S. Oganesyan, O. H. S. Ollila, et al., Phys. Chem. Chem. Phys. **18**, 32560 (2016).
[34] J. L. Browning and J. Seelig, Biochemistry **19**, 1262 (1980).
[35] F. Borle and J. Seelig, Chemistry and Physics of Lipids **36**, 263 (1985).
[36] J. Seelig and H. U. Gally, Biochemistry **15**, 5199 (1976).
[37] N. Michaud-Agrawal, E. J. Denning, T. B. Woolf, and O. Beckstein, Journal of Computational Chemistry **32**, 2319 (2011), https://onlinelibrary.wiley.com/doi/pdf/10.1002/jcc.21787, URL https://onlinelibrary.wiley.com/doi/abs/10.1002/jcc.21787.
[38] Richard J. Gowers, Max Linke, Jonathan Barnoud, Tyler J. E. Reddy, Manuel N. Melo, Sean L. Seyler, Jan Domaski, David L. Dotson, Sbastien Buchoux, Ian M. Kenney, et al., in *Proceedings of the 15th Python in Science Conference*, edited by Sebastian Benthall and Scott Rostrup (2016), pp. 98 – 105.
[39] P. G. Scherer and J. Seelig, Biochemistry **28**, 7720 (1989).
[40] I. Pascher, M. Lundmark, P.-G. Nyholm, and S. Sundell, Biochim. Biophys. Acta **1113**, 339 (1992).
[41] J. Seelig, P. M. MacDonald, and P. G. Scherer, Biochemistry **26**, 7535 (1987).
[42] J. Melcr, T. M. Ferreira, P. Jungwirth, and O. H. S. Ollila, Journal of Chemical Theory and Computation **16**, 738 (2020).
[43] L. shar Huang, D. Cobessi, E. Y. Tung, and E. A. Berry, Journal of Molecular Biology **351**, 573 (2005), ISSN 0022-2836, URL https://www.sciencedirect.com/science/article/pii/S0022283605006078.
[44] G. Schaaf, E. A. Ortlund, K. R. Tyeryar, C. J. Mousley, K. E. Ile, T. A. Garrett, J. Ren, M. J. Woolls, C. R. Raetz, M. R. Redinbo, et al., Molecular Cell **29**, 191 (2008), ISSN 1097-2765, URL https://doi.org/10.1016/j.molcel.2007.11.026.
[45] K. Muramoto, K. Ohta, K. Shinzawa-Itoh, K. Kanda, M. Taniguchi, H. Nabekura, E. Yamashita, T. Tsukihara, and S. Yoshikawa, Proceedings of the National Academy of Sciences **107**, 7740 (2010), ISSN 0027-8424, https://www.pnas.org/content/107/17/7740.full.pdf, URL https://www.pnas.org/content/107/17/7740.
[46] K. Tanaka, J. M. Caaveiro, K. Morante, J. M. González-Mañas, and K. Tsumoto, Nature Communications **6**, 6337 (2015), ISSN 2041-1723, URL https://doi.org/10.1038/ncomms7337.

ToDo